Reactions of H_2, CO, and O_2 with Active [NiFe]-Hydrogenase from *Allochromatium vinosum*. A Stopped-Flow Infrared Study†

Simon J. George,‡,# Sergei Kurkin,§,# Roger N. F. Thorneley,‡ and Simon P. J. Albracht*,§

Department of Biological Chemistry, John Innes Centre, Norwich Research Park, Colney, Norwich NR4 7UH, United Kingdom, and Swammerdam Institute for Life Sciences, Biochemistry, University of Amsterdam, Plantage Muidergracht 12, NL-1018 TV Amsterdam, The Netherlands

Received January 20, 2004; Revised Manuscript Received March 26, 2004

ABSTRACT: The Ni−Fe site in the active membrane-bound [NiFe]-hydrogenase from *Allochromatium vinosum* can exist in three different redox states. In the most oxidized state (Ni_a-S) the nickel is divalent. The most reduced state (Ni_a-SR) likewise has Ni^{2+}, while the intermediate state (Ni_a-C*) has Ni^{3+}. The transitions between these states have been studied by stopped-flow Fourier transform infrared spectroscopy. It is inferred from the data that the Ni_a-S → Ni_a-C* and Ni_a-C* → Ni_a-SR transitions induced by dihydrogen require one of the [4Fe-4S] clusters to be oxidized. Enzyme in the Ni_a-S state with all of the iron-sulfur clusters reduced reacts with dihydrogen to form the Ni_a-SR state in milliseconds. By contrast, when one of the cubane clusters is oxidized, the Ni_a-S state reacts with dihydrogen to form the Ni_a-C* state with all of the iron-sulfur clusters reduced. The competition between dihydrogen and carbon monoxide for binding to the active site was dependent on the redox state of the nickel ion. Formation of the Ni_a-S·CO state (Ni^{2+}) by reacting CO with enzyme in the Ni_a-SR and Ni_a-S states (Ni^{2+}) is considerably faster than its formation from enzyme in the Ni_a-C* (Ni^{3+}) state. Excess oxygen converted hydrogen-reduced enzyme to the inactive Ni_r* state within 158 ms, suggesting a direct reaction at the Ni−Fe site. With lower O_2 concentrations the formation of intermediate states was observed. The results are discussed in the light of the present knowledge of the structure and mechanism of action of the *A. vinosum* enzyme.

Hydrogenases catalyze the reversible reaction $H_2 \leftrightarrow 2H^+ + 2e^-$. They are widespread in nature. An introduction to [NiFe]-hydrogenases in general and to the membrane-bound enzyme from *Allochromatium vinosum* in particular is given in the accompanying paper in this issue (*1*). In that paper, the first stopped-flow Fourier transform infrared (SF-FTIR)[1] experiments on any hydrogenase were described that focused on the kinetics of the *inactive A. vinosum* enzyme with H_2, or H_2 in combination with CO or O_2. In the present paper, we report on the kinetics of some of the reactions of the *active A. vinosum* hydrogenase with a variety of reagents (a.o. H_2, CO, BV, and O_2) again using the SF-FTIR technique (*2*−*4*).

The Ni−Fe site in active enzyme can exist in three different states, designated Ni_a-S, Ni_a-C*, and Ni_a-SR. In the presence of mediating redox dyes plus H_2, the Ni_a-S → Ni_a-C* transition is reversible and involves one electron and two protons (*5*). This transition also occurs with hydrogen alone (no mediating dyes present), but then it is irreversible (*6*−*8*). The transition is not accompanied by any shift of the ν(CN) bands, but the ν(CO) band shifts some 17−20 cm^{-1} to higher frequency. Studies with the H_2-sensing protein from *Ralstonia eutropha* suggest that this transition is simply due to the binding of H_2 to the Ni_a-S state, whereby the Ni^{2+} is oxidized to Ni^{3+} (with the electron transferred to the Fe−S clusters) to form the Ni_a-C* state (*9*, *10*).

Below 77 K, the Ni_a-C* state converts to the Ni_a-L* state upon illumination with white light (*6*). As this conversion was slowed nearly 6-fold when performed in a D_2/D_2O environment, it has been interpreted as the photolysis of a hydrogen species bound to the active site. It is now generally assumed that the Ni_a-C* state contains a hydride bound to the active site in a position bridging between Ni and Fe (*11*, *12*).

Carbon monoxide is a competitive inhibitor of nearly all [NiFe]-hydrogenases. EPR studies have shown that CO binds directly to nickel when H_2-reduced enzyme is treated with limiting amounts of CO (*13*−*15*). The resulting Ni_a*·CO state (*16*) is converted to the Ni_a-L* state upon illumination. Although it was initially thought that CO and the light-sensitive H-species were bound to the same site on nickel (*6*, *14*), later studies with the *A. vinosum* enzyme suggested that the H-species (hydride) may be bound to the Fe site, while the CO binds to the nickel (*16*). When active enzyme is treated with excess CO, an EPR-silent state is obtained (Ni_a-S·CO). FTIR studies showed the binding of externally added CO to the active site in this state (*17*). The crystal structure of a CO-inhibited enzyme has been published (*18*)

† This work was supported by funds from the The Netherlands Organization for Scientific Research (NWO), Division for Chemical Sciences (CW), and by the UK Biotechnology and Biological Sciences Research Council who also funded the development of the SF-FTIR apparatus used in these studies.

* To whom correspondence should be addressed: Phone: +31 20 5255130; fax: +31 20 5255124; e-mail: asiem@science.uva.nl.

§ John Innes Centre.

‡ University of Amsterdam.

# These authors contributed equally to this work.

[1] Abbreviations: BV, benzyl viologen; MV, methyl viologen; FTIR, Fourier transform infrared spectroscopy; SF-FTIR, stopped-flow FTIR.

10.1021/bi049853k CCC: $27.50
Published on Web 05/06/2004

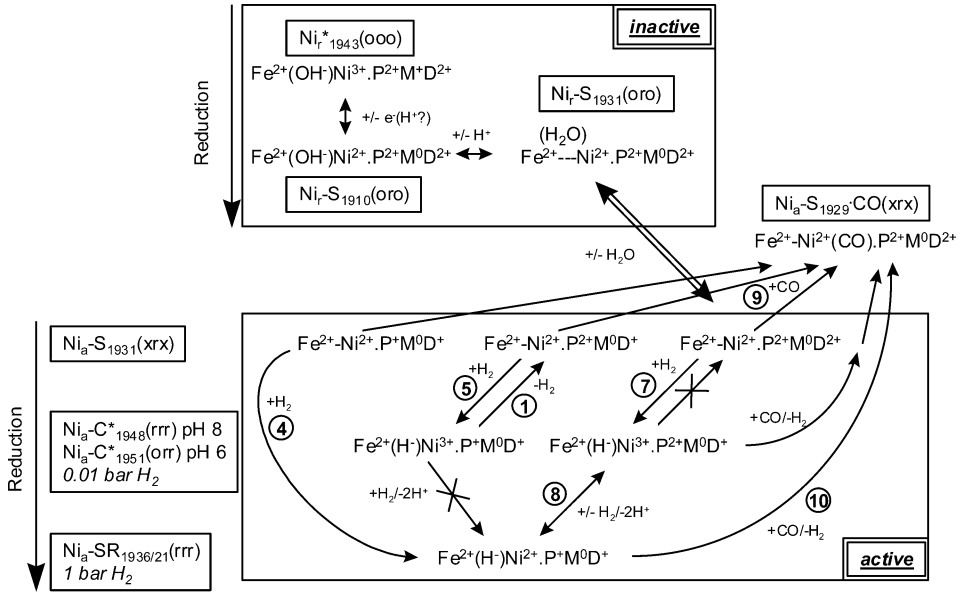

FIGURE 1: Overview of the redox states and their short-hand notations of the *A. vinosum* enzyme as studied in this paper. The reader may first wish to consult Figures 1 and 2 in the accompanying paper in this issue (*1*) as an introduction. The scheme should facilitate the understanding of the experiments in this study. The subscripts u, r, and a stand for unready, ready, and active, respectively. States marked with an asterisk (*) show a S = 1/2 EPR signal due to nickel. EPR-silent states have an S added; SR stands for silent reduced. The number added to each state as a subscript represents the stretching frequency of the intrinsic CO bound to Fe. Also the status of the Fe−S clusters is indicated. For example, the oxidized ready state can be written as $Fe^{2+}(OH^-)Ni^{3+}{\cdot}P^{2+}M^+D^{2+}$, where OH^- stands for the bridging oxygen species, P^{2+} for the oxidized proximal $[4Fe\text{-}4S]^{2+}$ cluster, M^+ for the oxidized medial $[3Fe\text{-}4S]^+$ cluster, and D^{2+} for the oxidized distal $[4Fe\text{-}4S]^{2+}$ cluster. In the text, we will also refer to this state as Ni_r*(ooo), where "o" stands for an oxidized Fe−S cluster, and "r" stands for a reduced cluster (order: proximal, medial, distal). If an "x" is used, the cluster can be either oxidized or reduced. Many of the conclusions of the present paper have been integrated already into the scheme. Under 1 bar of H_2, the enzyme is mainly in the Ni_a-SR states with ν(CO) bands at 1936 and 1921 cm^{-1} (two pH-dependent substates). This state can be written as $Fe^{2+}(H^-)Ni^{2+}{\cdot}P^+M^0D^+$, where H^- stands for a bound hydride (light sensitive in the Ni_a-C* state). Other states are observed at higher redox potentials. *Note that the Ni_r-S_{1910}, Ni_r-S_{1931}, and Ni_a-S_{1931} states are isopotential*. The mobility of the H_2O molecule in the Ni_r-S_{1931} state, proposed to be formed by protonation of the bridging OH^- in the Ni_a-S_{1910} state, is assumed to be strongly temperature dependent. At 2 °C, it cannot leave the active-site pocket and blocks the binding of H_2. Binding of H_2 would result in the Ni_a-C* state, which has a hydride in the bridging position. Also, at 2 °C it is assumed that a water molecule cannot enter the empty active-site pocket in the (active) Ni_a-S_{1931} state. At 25 °C, these restrictions are far less stringent, enabling a rapid equilibrium between the Ni_r-S_{1931} and Ni_a-S states. The ν(CO) band of the Ni_a-C* state can slightly shift depending on the redox state of the proximal cluster (*34*). This shift could not be observed in the present study due to a lower resolution; changes at 1950 cm^{-1} are assigned to the Ni_a-C* state. Encircled numbers relate to the equations in the text.

and shows that CO is bound to nickel opposite to the bridging thiol provided by the last Cys residue in the C-terminus of the large subunit (S_{533} in Figure 1 of the accompanying paper in this issue (*1*)).

The Ni_a-C* state, with a bound hydride, reacts with a second dihydrogen molecule to form the EPR-silent Ni_a-SR state. The reaction $Ni_a\text{-}C^* + H_2 \Leftrightarrow Ni_a\text{-}SR$ is the *only equilibrium reaction* ($n = 2$, $1H^+/e^-$) involving hydrogen and the enzyme in the absence of redox mediators (*7*).

The turnover rate of active *A. vinosum* [NiFe]-hydrogenase with H_2 is extremely high. When attached to a pyrolytic graphite electrode, the turnover rate is in the range of 1500−9000 s^{-1} at 30 °C (*19*, *20*) and is limited by H_2 diffusion from the bulk solution to the enzyme. This means that the primary reaction of active enzyme with H_2 lies outside the time resolution of conventional rapid-mixing techniques, such as that used in the SF-FTIR apparatus. The objective of the present paper was therefore to investigate the reactions of the active enzyme with hydrogen, carbon monoxide, and oxygen, starting from the three well-defined active states: Ni_a-S, Ni_a-C*, and Ni_a-SR. Some of these reactions had been studied earlier by rapid-mixing rapid-freezing EPR (*16*). Since the Ni-EPR signal is absent in two of the active states, the study by SF-FTIR was expected to provide more detailed and conclusive information, and this was indeed the case. In addition, some reactions were predicted to be quite slow (seconds to minutes), and so they were unsuited for the available discontinuous rapid-mixing EPR technique due to the very large amounts of enzyme required (*16*). Continuous detection of these reactions by SF-FTIR enabled the verification of such predictions.

The results reported below together with those in the accompanying paper (*1*) substantially increase our understanding of the interrelationships between the several states of this extremely complicated enzyme system.

EXPERIMENTAL PROCEDURES

Enzyme Purification and Sample Preparation. The *A. vinosum* [NiFe]-hydrogenase (specific H_2-benzyl viologen activity at pH 8 and 30 °C: 300 U/mg) was prepared as described (*21*). Enzyme, dissolved in 50 mM Tris-HCl buffer (pH 8.0), was concentrated to 80−90 μM by ultrafiltration and stored at −80 °C. This preparation and buffer were used throughout unless specified otherwise. The reduced, active enzyme in the Ni_a-SR state was obtained by an incubation under 1 bar H_2 at 50 °C for 30 min in a capped serum bottle. Unless specified otherwise, the Ni_a-C* state was prepared by transferring the bottle into the anaerobic box of the SF-FTIR apparatus and exposing the contents to the gas atmosphere in the box (N_2 with maximally 2 ppm O_2) for 30 min at room temperature. The Ni_a-S state was obtained

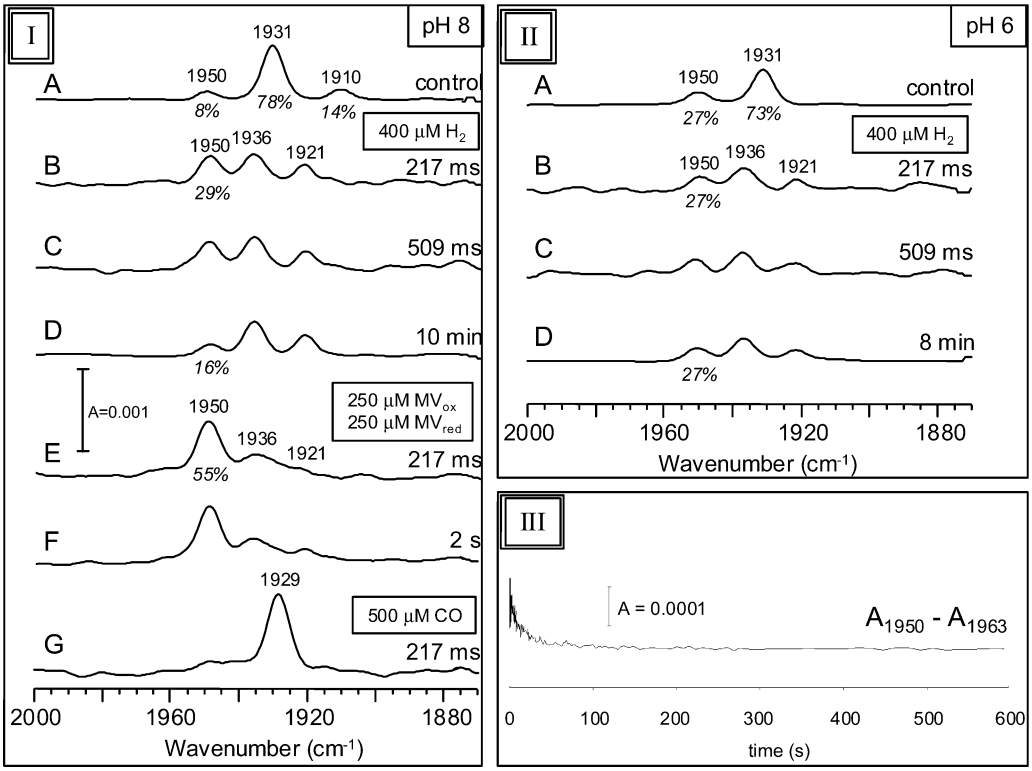

FIGURE 2: Reaction of enzyme in the Ni_a-S state with H_2, reduced MV or CO. Syringe 1 contained enzyme in the Ni_a-S state in buffer of pH 8 (panel I) or 6 (panel II). (A) Control experiments: enzyme was mixed (1:1 v/v) with anaerobic buffer. A spectrum was recorded 3 min after mixing. (B−D) Syringe 2 contained buffer with 800 μM H_2 and spectra were obtained after 217 ms (B), 509 ms (C) and 8 min (II, D) or 10 min (I, D). (E, F) Syringe 2 contained buffer (pH 8) with 1000 μM 50%-reduced MV. Spectra were recorded after 217 ms (E) and 2 s (F). (G) Syringe 2 was filled with buffer (pH 8) containing 1000 μM CO; 217 ms after mixing a spectrum was obtained. (Panel III) Time dependence of the amplitude of the 1950 cm^{-1} band for the experiment under I, B−D. The absorbance at 1963 cm^{-1} was used as an internal reference. All spectra were baseline corrected. Only the υ(CO) region is shown. Concentrations given in the figures are those after mixing.

by recapping the serum bottle and leaving it for 18 h in the anaerobic box at room temperature. At pH 6, this procedure did not work; the Ni_a-C* state persisted even after 1 day. Therefore, at pH 6.0 the Ni_a-S state was prepared by mixing enzyme (80−90 μM) in the Ni_a-C* state in a capped serum bottle with air-saturated buffer to a final O_2 concentration of 25 μM. The actual state (or mixture of states) of the enzyme at the start of each experiment was determined by FTIR. The different concentrations of CO, H_2, or O_2 and their mixtures were obtained as described in the accompanying paper (*1*). A 50% reduced solution of 1 mM MV was prepared electrochemically (*22*).

SF-FTIR Measurements and Data Analysis. SF-FTIR experiments were performed as described in the accompanying paper (*1*). The enzyme syringe (syringe 1) contained hydrogenase (80−90 μM) preconditioned as described in the text. The reactant syringe (syringe 2) contained the buffer at the appropriate pH with the additions specified in the text. Both syringes were of equal size and their contents were mixed in a 1:1 (v/v) ratio.

RESULTS AND DISCUSSION

Explanatory Scheme to Facilitate the Understanding of the Experimental Design and Discussions. Before describing the experimental observations, it is important to recall that the Ni−Fe site in the *A. vinosum* hydrogenase behaves as an $n = 1$ redox entity. Hence, in the two-electron reaction with H_2, the redox states of the Fe−S clusters must also be taken into consideration (*7*). All [NiFe]-hydrogenases have only the proximal [4Fe-4S] cluster in common, suggesting that this cluster is essential for the redox reaction with H_2 (*23*). The scheme in Figure 1 gives an overview of some of the reactions investigated in this study. As far as the active enzyme is concerned, this scheme is more detailed than that in the accompanying paper (*1*), because many of the conclusions from the present paper are included. The redox states of the Fe−S clusters are included in the descriptions of the various enzyme states. In this paper, we will use the short-hand notations as described in detail in the legend to Figure 1.

Reactions of Enzyme in the Ni_a-S State. At pH 8 and pH 6 the Ni_a-S state was prepared as described in Experimental Procedures. When mixed with anaerobic buffer at pH 8 the spectrum shown in Figure 2I, trace A was obtained. The main υ(CO) band was at 1931 cm^{-1} (78% of the total υ(CO) intensity), with smaller bands at 1950 cm^{-1} (Ni_a-C*; 8%) and 1910 cm^{-1} (Ni_r-S_{1910}; 14%). At pH 6, only the 1950 cm^{-1} (27%) and 1931 cm^{-1} (73%) bands were observed (Figure 2II, trace A).

At pH 8, the small υ(CO) bands at 1950 and 1910 cm^{-1} and the large 1931 cm^{-1} band show that the bulk of the enzyme is in a state between the Ni_a-C* and the Ni_r-S_{1910} states, i.e., the Ni_a-S and Ni_r-S_{1931} states (see Figure 1). At pH 6, the 1910 cm^{-1} band was not detectable, presumably due to protonation of the Ni_r-S_{1910} state (Figure 1). As the Ni_r-S_{1931} and Ni_a-S states are easily interconvertible at 25

°C and have the same infrared spectrum, they cannot be distinguished here. When prepared at 2 °C, the Ni_r-S_{1910}/Ni_r-S_{1931} states are not active. In an activity assay at 30 °C, such a preparation requires several seconds to become active (*24*).

(a) Reaction of the Ni_a-S State with H_2 at pH 8 and 6. When enzyme (at pH 8) was mixed with buffer containing 800 μM H_2, the 1931 cm^{-1} band disappeared within 217 ms (Figure 2I, traces A and B). Two other bands characteristic of the Ni_a-SR states (1936 cm^{-1}, 1921 cm^{-1}, 71%) appeared, while the 1950 cm^{-1} band increased (Ni_a-C*, 29%). At 509 ms, the spectrum was essentially the same. At longer times (up to 100 s), a slow decrease of the 1950 cm^{-1} band was observed (Figure 2I, trace D, and 2III). The same experiment performed at pH 6 resulted in the complete conversion within 217 ms of the 1931 cm^{-1} band into bands at 1936/1921 cm^{-1} characteristic of the Ni_a-SR states. The 1950 cm^{-1} band did not change in intensity. There were no further changes at longer times (Figure 2II, traces A−D).

It is concluded that under the above conditions, the reaction of H_2 with enzyme mainly in the Ni_a-S/Ni_r-S_{1931} states was complete within 217 ms at both pH 8 and 6. In both cases, the Ni_a-SR states were the main products. The fast (217 ms) increase of Ni_a-C* (from 8 to 29%) at pH 8, and its subsequent slow decrease ($t_{1/2}$ = 6 s), as well as the absence of this effect at pH 6 were unexpected observations.

To understand this behavior, it is important to recall how the Ni_a-S state at both pH values was prepared. At pH 8, it was obtained from the Ni_a-C* state by leaving the enzyme in an H_2-free, anaerobic atmosphere for 18 h at room temperature. This resulted in the spectrum of Figure 2I, trace A. EPR and Mössbauer spectra of the active *A. vinosum* enzyme at pH 8 under 1 or 0.01 bar of H_2 showed that all of the Fe−S clusters are reduced under both conditions, i.e., one $[3Fe\text{-}4S]^0$ cluster and two $[4Fe\text{-}4S]^+$ clusters (*25*, *26*). Hence, at pH 8 a Ni_a-C*(rrr) state was present at the start of the Ni_a-S preparation procedure.

Studies with the H_2-sensing, regulatory hydrogenase (RH) from *R. eutropha* indicate that the reaction of the Ni_a-S state with H_2 involves only H_2 binding to the active site, whereby the Ni^{2+} is oxidized to Ni^{3+} and an electron is passed onto the Fe−S clusters and from there to an as yet unidentified *n* = 2 redox-active chromophore (*9*, *10*). By analogy, we propose that the formation of the Ni_a-S state in the *A. vinosum* enzyme from the Ni_a-C* state can be written as the reverse of this reaction (eq *1*).

$$Fe^{2+}(H^-)Ni^{3+}\cdot P^+M^0D^+ + H^+ \rightarrow Fe^{2+}\text{-}Ni^{2+}\cdot P^{2+}M^0D^+ + H_2 \quad (1)$$

i.e.. a very slow (18 h) release of H_2 from the active site, whereby Ni^{3+} is reduced to Ni^{2+} using an electron from the cubane with the lowest midpoint potential. In short, this can be written as Ni_a-C*(rrr) → Ni_a-S(orr) + H_2 (see Figure 1).

EPR experiments showed that the cubane clusters remained largely reduced when performing this treatment (*27*), implying that the proximal cluster in a large proportion of the enzyme becomes re-reduced. We are not sure how this occurs. Equation 1 shows that the amount of H_2 released is stoichiometric with respect to the enzyme. However, by equilibration with the gas phase in the serum bottle, the H_2 concentration in the solution will decrease to 3−4 orders of magnitude lower than that of the enzyme. We suggest that the released H_2 could be the source of electrons for the slow reduction of the oxidized proximal cluster (eqs 2 and 3).

$$Ni_a\text{-}S(orr) + Ni_a\text{-}S(orr) \Leftrightarrow Ni_a\text{-}S(oro) + Ni_a\text{-}S(rrr) \quad (2)$$

$$Ni_a\text{-}S(oro) + H_2 \rightarrow Ni_a\text{-}S(rrr) + 2H^+ \quad (3)$$

Thus, the main products of the procedure to make the Ni_a-S state at pH 8 are expected to be Ni_a-S(rrr) and Ni_a-S(orr) with both exhibiting a 1931 cm^{-1} band (Figure 2I, trace A).

Formation of the Ni_a-SR states (1936/1921 cm^{-1} bands) by reaction of enzyme in the Ni_a-S(rrr) state with 400 μM H_2 is expected to be fast (eq 4).

$$Ni_a\text{-}S(rrr) + H_2 \rightarrow Ni_a\text{-}SR(rrr) + H^+ \quad (4)$$

i.e., the fast binding of H_2 (as hydride) to the active site (Figure 1). Hydrogen (hydride) binding to the Ni_a-S(orr) state, however, will result in the formation of the Ni_a-C*(rrr) state (eq *5*).

$$Fe^{2+}\text{-}Ni^{2+}\cdot P^{2+}M^0D^+ + H_2 \rightarrow Fe^{2+}(H^-)Ni^{3+}\cdot P^+M^0D^+ + H^+ \quad (5)$$

In this case, formation of an $Fe^{2+}(H^-)Ni^{3+}\cdot P^+M^0D^+$ species is preferred over the formation of an $Fe^{2+}(H^-)Ni^{2+}\cdot P^{2+}M^0D^+$ species, because the midpoint potential of the Ni^{3+}/Ni^{2+} couple in the Ni_a-C*/Ni_a-SR transition is lower than that of the P^{2+}/P^+ couple (*5*). We suggest that this may be due to differences in the bonding interactions of the H^- ion with the Fe^{2+}-Ni^{3+} and Fe^{2+}-Ni^{2+} centers. Such an interaction will be determined by oxidation levels, electron distribution, and the protein environment of the Fe−Ni cluster. The Ni_a-C*-(rrr) state will not be reduced by H_2 as it has only one oxidizing equivalent available (see below). This is how we explain the behavior of the 1950 cm^{-1} band in Figures 2-I, A−D and 2-III. A complete redox equilibrium between all of the enzyme states and 400 μM H_2 was obtained in a reaction with a $t_{1/2}$ of 6 s (Figure 2III). This slow phase is assigned to intermolecular reactions between different enzyme forms (*28*). The rapid disappearance of the 1910 cm^{-1} band (Ni_r-S_{1910} state) with H_2 can be understood as follows. We assume that the Ni_r-S_{1910} state still has an OH^- bridge between Ni and Fe (Figure 1). Protonation to water leads to the Ni_r-S_{1931} state. If at 25 °C, this H_2O molecule is considered to be highly mobile, then the Ni_r-S_{1931} (with water) and Ni_a-S_{1931} (no water) states can rapidly interconvert. Water leaving the active-site pocket will allow hydrogen to rapidly occupy the bridging position (as a hydride) to form the stable Ni_a-C* state (Figure 1). In contrast to active enzyme, enzyme in the Ni_r-S states is not active in the H_2-methylene blue assay (*24*).

Previous EPR experiments at pH 6 showed that under 1% H_2, 90% of the enzyme is in the Ni_a-C* state, but with the proximal cluster largely oxidized (Ni_a-C*(orr) state) (*7*, *26*). In the present study, we observed that the Ni_a-C* state persisted at pH 6 for at least 1 day in the absence of H_2. The presence of the oxidized proximal cluster may be the reason this state is so stable at this pH, i.e., because the reaction shown in eq 1 cannot occur. Abstraction of the

required electron from the distal cluster is probably prevented by the higher redox potential of this cluster. This is why 25 μM O_2 was used to remove reducing equivalents from the enzyme. A plausible reaction for the formation of the Ni_a-S state by this method is the removal of the H-species by oxidation with oxygen (eq 6).

$$Fe^{2+}(H^-)Ni^{3+}\cdot P^{2+}M^0D^+ + 0.5O_2 + H^+ \rightarrow Fe^{2+}\text{-}Ni^{2+}\cdot P^{2+}M^0D^{2+} + H_2O \quad (6)$$

As the enzyme concentration was 80−90 μM, the bound H_2 is expected to be removed in at least half of the enzyme molecules. Figure 2II, trace A shows that 73% of the enzyme is in the Ni_a-S state (1931 cm^{-1} band), which is in good agreement with this prediction. Reaction of the Ni_a-S(oro) state with excess H_2 can rapidly yield the Ni_a-SR(rrr) state, as depicted in eqs *7* and *8*.

$$Fe^{2+}\text{-}Ni^{2+}\cdot P^{2+}M^0D^{2+}H_2 \rightarrow Fe^{2+}(H^-)Ni^{3+}\cdot P^{2+}M^0D^+ + H^+ \quad (7)$$

$$Fe^{2+}(H^-)Ni^{3+}\cdot P^{2+}M^0D^+ + H_2 \rightarrow Fe^{2+}(H^-)Ni^{2+}\cdot P^{+}M^0D^+ + 2H^+ \quad (8)$$

Thus, initially H_2 binds to Ni_a-S(oro) to form Ni_a-C*(orr) and then a second H_2 molecule reduces the Ni^{3+} ion and the proximal cluster to form Ni_a-SR(rrr) (see also Figure 1). This is what is observed in Figure 2II. The Ni_a-S_{1931}(oro) to Ni_a-$SR_{1936/21}$(rrr) transition was completed within 217 ms.

Curiously, the intensity of the 1950 cm^{-1} band (Ni_a-C*), about 27% at the start of the reaction, did not change with time. There are two possible explanations: (i) the Ni_a-C* state had all cubanes reduced (i.e., the Ni_a-C*(rrr) state), preventing a rapid reaction with H_2; (ii) one cubane was oxidized (Ni_a-C*(orr) state), enabling a rapid (ms) equilibrium with the Ni_a-SR(rrr) state. This equilibrium happened to result in 27% Ni_a-C*, as apparent from the spectrum at 8 min. Since oxygen was used to produce the starting mixture of states, we favor the second explanation.

(b) Reaction of the Ni_a-S State with Reduced Methyl Viologen. The reaction of the Ni_a-S state (at pH 8) with electrochemically reduced MV is shown in Figure 2I, traces E and F. These conditions are analogous to those used for the H_2-production assay, except for the higher reduced MV concentration and the presence of dithionite in the assay. With final concentrations at the start of the reactions of 250 μM reduced and 250 μM oxidized MV, the reaction will approach an equilibrium determined by the relative concentrations of reduced and oxidized MV (initially −449 mV), the pH, and the dihydrogen formed. Hence, formation of a mixture of the Ni_a-C* and Ni_a-SR states was expected, and this is what was observed. Within 217 ms, the Ni_a-S/Ni_r-S_{1931} and Ni_r-S_{1910} states had completely disappeared with concomitant formation of a stable mixture of the Ni_a-C* (55%) and Ni_a-SR (45%) states.

(c) Reaction of the Ni_a-S State with CO. Figure 2I, trace G shows the spectrum taken 217 ms after mixing enzyme (80 μM) in the Ni_a-S state at pH 8 with buffer saturated with CO (1000 μM). One strong υ(CO) band at 1929 cm^{-1} is apparent. In addition, three weaker bands were seen (not shown): one υ(CO) band from the extrinsic CO bound to nickel (2054 cm^{-1}) and two υ(CN) bands (2080 and 2068 cm^{-1}). All of these bands are characteristic of the Ni_a-S·CO state. For the Ni_a-S state, the reaction with CO can be written as eq *9*.

$$Ni_a\text{-}S(rrr) + CO \rightarrow Ni_a\text{-}S\cdot CO(rrr) \quad (9)$$

The starting sample (Figure 2I, trace A) also contained some Ni_a-C* (1950 cm^{-1}) and Ni_r-S_{1910} (also probably some Ni_r-S_{1931}, but this cannot be distinguished from Ni_a-S_{1931}). Apart from the redox states of the cubane clusters, the reactions of Ni_a-C* can be explained by eqs 1 and 9. A discussion of the kinetics of the Ni_a-C* to Ni_a-S·CO transition is given later.

The rate of reaction of the Ni_r-S states with CO is proposed to be limited by the loss of H_2O from the active site pocket as discussed for the reaction with H_2 (Figure 1). We note that when the Ni_r-S states are prepared at 2 °C, they only react very slowly (tens of minutes) with CO, the rate presumably being limited by the slow release of the water molecule at this temperature (Bleijlevens, B., and Albracht, S. P. J., unpublished experiments).

Reactions of Enzyme in the Ni_a-C State.*

(a) Reaction with H_2 at pH 8 and 6. Redox titrations with H_2/He mixtures (*7*) showed that Ni_a-C* (with Ni^{3+}) and Ni_a-SR (with Ni^{2+}) are in an $n = 2$ redox equilibrium: Ni_a-C* + $H_2 \leftrightarrow Ni_a$-SR. Because the 3Fe cluster ($E_0' = -10$ mV, pH 8) is always reduced in active enzyme, one of the [4Fe-4S] clusters must be involved in this equilibrium (*7*). As remarked above, all of the Fe−S clusters remained reduced in both states at pH 8. The reason for this apparent contradiction is that under such equilibrium conditions, intermolecular electron exchange will produce a mixture of states in equilibrium with the potential set by the H_2-partial pressure (*28*). The situation is different, however, in a kinetic experiment in which the Ni_a-C* state reacts with H_2. At pH 8, our preparation protocol will ensure that the main part of the Fe−S clusters in the Ni_a-C* state are reduced. Since only one more electron can be accommodated by this state (at Ni^{3+}), the reaction with H_2 is expected to be slow. This could explain why the reaction with H_2 with the formed Ni_a-C* in Figure 2III is so slow.

To substantiate this explanation, enzyme in the Ni_a-C* state at pH 8 was prepared by equilibrating H_2-reduced enzyme with the N_2 gas in the glovebox for 30 min at 25 °C. A control experiment in which this enzyme was mixed with anaerobic buffer produced a spectrum with a strong 1950 cm^{-1} band (Ni_a-C*; 63%; Figure 3.I, A), while 37% was still in the Ni_a-SR states (1936 and 1921 cm^{-1} bands). This is close to the value obtained with EPR experiments under similar conditions (1% H_2 in the gas phase), where up to 60% of the enzyme can be obtained in the Ni_a-C* state at pH 8 and 90% at pH 6 (*7*, *26*). After the sample was mixed with H_2-saturated buffer (400 μM H_2 after mixing), the 1950 cm^{-1} band decreased to 35% within 158 ms, whereas the 1936 and 1921 cm^{-1} bands increased to 65% (Figure 3I, trace B). As this spectrum had a distorted baseline, we show the spectrum obtained at 276 ms, which was of better quality. This fast phase was followed by a slow phase ($t_{1/2} = 6$ s) during which the 1950 cm^{-1} band decreased to 14%. The time-dependent amplitude changes of the 1950, 1936, and

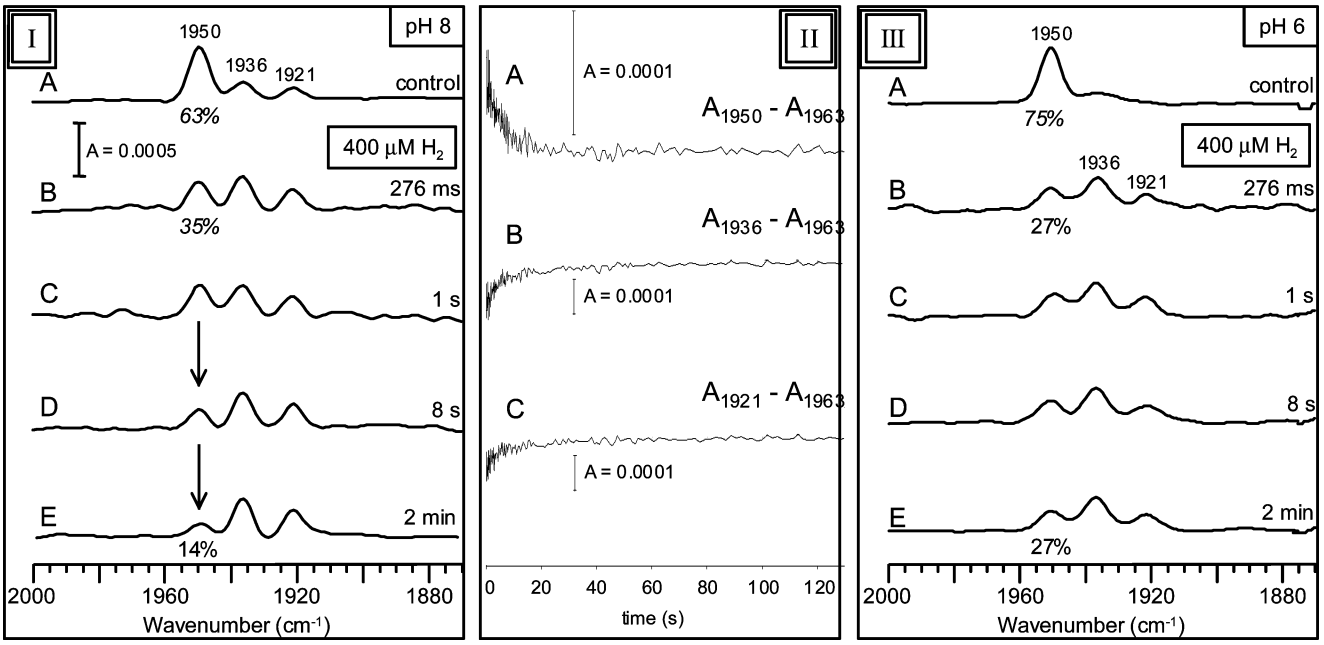

FIGURE 3: The reaction of H_2 with enzyme in the Ni_a-C* state at pH 8 (I, II) or pH 6 (III). Syringe 1 contained enzyme in the Ni_a-C* state; syringe 2 contained buffer with 800 μM H_2. Panels I and III: (A) Controls with syringe 2 filled with anaerobic buffer; a spectrum was taken after 3 min. (B−E) Reaction with H_2 after 276 ms (B), 1 s (C), 8 s (D), and 2 min (E). Panel II: Time dependence of the amplitudes of the 1950 (A), 1936 (B), and 1921 cm^{-1} bands (C) in the experiment in panel I. The absorbance at 1963 cm^{-1} was used as reference.

1921 cm^{-1} bands are plotted in Figure 3II. The 1936/1921 bands increased concomitantly with the decrease of the 1950 cm^{-1} band.

At pH 6 the proximal [4Fe-4S] cluster is largely oxidized in enzyme equilibrated under 1% H_2; hence, it was anticipated that at this pH the reaction with excess H_2 might show different kinetics. An anaerobic control showed that 75% of the enzyme was in the Ni_a-C* state (Figure 3III, trace A) in good agreement with earlier EPR data (*7*, *26*). The infrared spectra show additionally that the rest of the enzyme remains in the (EPR-silent) Ni_a-SR states (1936/1921 cm^{-1} bands). After mixing with H_2-saturated buffer, the system reached equilibrium within 158 ms with only 27% Ni_a-C* present. The rest of the enzyme was in the Ni_a-SR state (Figure 3III, traces B−E).

The fast reaction can be explained by the fact that enzyme in the Ni_a-C* state at pH 6 comprises two oxidizing equivalents, Ni^{3+} and an oxidized proximal cluster. Hence, hydrogen can react very rapidly (milliseconds) to form the Ni_a-SR(rrr) state (eq 8). This also holds for the fast phase observed at pH 8 (Figure 3I, traces A and B). The slow phase in the decrease of the Ni_a-C* band (1950 cm^{-1}) at pH 8 (Figure 3I traces B−D and Figure 3II; see also Figure 2III) is due to the Ni_a-C*(rrr) state component present at the start of the reaction. Because only one oxidizing equivalent is present, reaction with H_2 cannot occur (Figure 1). Intermolecular electron exchange reactions are required to attain equilibrium. It is concluded that an oxidized proximal cluster is essential for a fast reaction or H_2 with the Ni_a-C* state.

(b) Reaction of the Ni_a-C State with Benzyl Viologen in the Presence of H_2.* To explore which states of the enzyme are involved in the catalytic cycle during the H_2−BV reaction, we have studied at pH 8 the reactions of enzyme mainly in the Ni_a-C* state (63%), with BV at different concentrations of H_2. On mixing 4 mM BV plus 80 μM H_2 with enzyme (80 μM), the small ν(CO) bands from the Ni_a-SR states disappeared within 100 ms (due to baseline disturbances, the 276 ms spectrum is shown), while the 1950 cm^{-1} band decreased to 26% of the total ν(CO) band intensity (Figure 4, trace B). At the same time a strong band at 1931 cm^{-1} appeared (Ni_a-S/Ni_r-S_{1931} states). No further changes were noticed during the next 3 min (Figure 4, trace C). The redox potential set by the H_2 concentration at the start of the reaction is −375 mV. The midpoint potential of BV is −358 mV, but at the start of the reaction the potential is at least 118 mV higher. Reduction of BV at the expense of H_2, catalyzed by the enzyme, will rapidly come to redox equilibrium. The experiment showed that equilibrium was reached within 100 ms. With 40 μM enzyme with a specific H_2−BV activity of 300 U/mg (pH 8, 30 °C), it is estimated that 40 μM H_2 can be consumed in a little more than 2 ms.

With 4 mM BV and 800 μM H_2 in the reactant syringe similar fast changes (<158 ms) were observed (Figure 4, traces D−F). In this case, the final potential was lower than in the previous experiment because the H_2 concentration was 10-fold higher. This resulted in more Ni_a-C* at equilibrium (61% Ni_a-C* and 39% Ni_a-S/Ni_r-S_{1931}). In all cases (Figure 4, traces B−F), the contribution of the Ni_a-SR states was negligible. We note that in FTIR redox titrations with the *Desulfovibrio gigas* enzyme in the presence of mediators, the Ni_a-C* and Ni_a-S states, but not the Ni_a-SR states, could be observed between −400 and −250 mV at pH 8.3 (*29*). This suggests that the final potential in our experiments was in that range. No slow reactions were observed in Figure 4, indicating that BV promotes rapid redox equilibration between all enzyme states. In both experiments, the H_2−BV reaction catalyzed by 40 μM enzyme was too fast to enable any intermediates to be detected.

(c) Reaction of the Ni_a-C State with CO.* This reaction was studied with 100 and 500 μM CO (final concentrations) at pH 8. With 100 μM, CO the Ni_a-SR states (1936/1921 cm^{-1}) disappeared within 100 ms (Figure 5I, traces A and

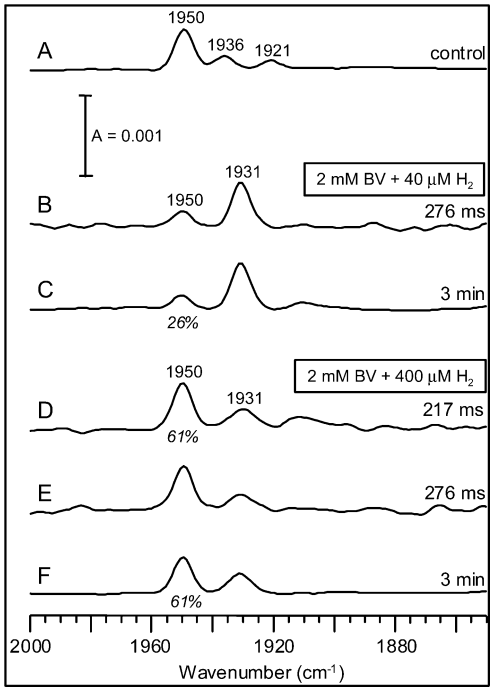

FIGURE 4: Reactions of enzyme in the Ni_a-C* state at pH 8 with 4 mM BV plus two different H_2 concentrations. Syringe 1 was filled with enzyme in the Ni_a-C* state. Syringe 2 contained buffer with 4 mM BV and 80 or 800 μM H_2. (A) Control experiment where the enzyme was mixed with anaerobic buffer; the spectrum was recorded 3 min after mixing. (B, C) Syringe 2 contained buffer with 4 mM BV and 80 μM H_2. Spectra were taken after 276 ms (B) and 3 min (C). (D−F) Syringe 2 contained buffer with 4 mM BV and 800 μM H_2. Spectra were taken after 217 ms (D), 276 ms (E), and 3 min (F).

B) and a strong band at 1929 cm^{-1}, assigned to the Ni_a-S·CO state, appeared. At the same time, the intensity of the 1950 cm^{-1} band decreased from 63 to 31% of the total υ(CO) intensity. At longer times (276 ms), a slow further decrease of the 1950 cm^{-1} band occurred with a simultaneous increase in intensity of the 1929 cm^{-1} band (Figure 5I, traces C and D). The changes occurred with a $t_{1/2}$ of a ca. 4−6 s (Figure 5II). In the 2100−2050 cm^{-1} region, three other bands characteristic of the Ni_a-S·CO state appeared (2080, 2068, and 2054 cm^{-1}). The reaction with buffer containing 1000 μM CO gave essentially the same results, except that the changes were complete within 217 ms (the 276 ms trace is shown; Figure 5I, traces E and F).

The portion of enzyme in the Ni_a-SR(rrr) states, present at the start of the reaction, can react with CO according to eq 10.

$$Fe^{2+}(H^-)Ni^{2+}\cdot P^+M^0D^+ + CO + H^+ \rightarrow Fe^{2+}\text{-}Ni^{2+}(CO)\cdot P^+M^0D^+ + H_2 \quad (10)$$

The reaction of the Ni_a-C* state at pH 8 with CO is explained as the dissociation of H_2 (eq 1) induced by the binding of CO to form the Ni_a-S·CO(orr) state. With 500 μM CO the reaction was too fast to follow, but at 100 μM CO the 1950 cm^{-1} band decreased more slowly (Figure 5I, traces A−D). An explanation for the slow reaction is given later.

Reactions of Enzyme in the Ni_a-SR State.

(a) Decreasing the H_2 Concentration from 800 to 400 μM. When enzyme in buffer with 800 μM H_2 was mixed (1:1, v/v) with anaerobic buffer, the resulting spectrum was within error the same as the spectrum obtained after mixing with H_2-saturated buffer (800 μM H_2), and no intermediates were observed (not shown). The experiments performed in the present paper (at 25 °C) are considered to be better controlled than previously reported freeze-quench experiments, which, for unknown reasons, gave slightly different results (*16*).

(b) Reaction of the Ni_a-SR State with Benzyl Viologen in the Presence of H_2. Hydrogen-reduced enzyme was mixed with hydrogen-saturated buffer containing 4 mM BV (Figure 6). The bands of the Ni_a-SR states (1936/1921 cm^{-1}) disappeared completely and a strong υ(CO) band at 1950 cm^{-1} (and two υ(CN) bands at 2084 and 2073 cm^{-1}; not shown) assigned to the Ni_a-C* state (81%) appeared. A weak band at 1931 cm^{-1}, from the Ni_a-S/Ni_r-S_{1931} states, also appeared. The changes were complete within 158 ms and hence too fast for the SF-FTIR apparatus to obtain a time course (Figure 6D). Mixing with 10 mM BV plus 800 μM H_2 resulted in a small band at 1950 cm^{-1} and a strong band at 1931 cm^{-1}. At 100 ms, only one band at 1950 cm^{-1} was observed. Subsequently, this band decreased, and a 1931 cm^{-1} appeared. At 276 ms, the changes were complete (spectra not shown since they had large baseline drifts).

The rate of H_2 oxidation is expected to be faster with 5 mM BV than with 2 mM BV. The experiments with 2 mM BV shows that the reaction was in redox equilibrium within 158 ms, resulting in a large 1950 cm^{-1} band. With 10 mM BV, the equilibrium is expected to be reached even faster than this. Both results are in line with the prediction that 800 μM H_2 can be consumed by the enzyme (40 μM; specific activity 300 U/mg at pH 8 and 30 °C) in about 42 ms. With 5 mM BV the only state detectable at 100 ms was the Ni_a-C* state (1950 cm^{-1}); the Ni_a-S state (1931 cm^{-1}) appeared later and concomitantly the Ni_a-C* state largely disappeared. This is consistent with the view that during the experiment the Ni_a-SR and Ni_a-C* states remained in equilibrium with the rapidly decreasing H_2 concentration and that what we observed at 100 ms was simply the end point of a "hydrogen-depletion titration". Only after hydrogen in solution was completely consumed were the reducing equivalents associated with the bridging hydride transferred to BV. This is consistent with the assumption that under these conditions the Ni_a-SR→Ni_a-C* transition is faster than the Ni_a-C*→Ni_a-S transition. As mentioned earlier, the Ni_a-C* to Ni_a-S conversion is extremely slow (days) in the absence of mediators. In view of the size of BV, it is unlikely that it can enter the gas channel in the enzyme. Hence, the most likely reaction site is the exposed edge of the distal Fe−S cluster. Thus, the bridging hydride in the Ni_a-C* state can be rapidly oxidized when electrons are abstracted via the Fe−S clusters. The experiment supports the view that during the H_2−BV reaction cycling of the enzyme between the Ni_a-SR and Ni_a-C* states is the preferred mode of action.

(c) Reaction of the Ni_a-SR State with CO. Hydrogen-reduced enzyme (800 μM H_2) was mixed with a CO-saturated buffer (1000 μM CO). An essentially homogeneous spectrum (bands at 2080, 2068, 2054, and 1929 cm^{-1}), typical of the Ni_a-S·CO state, was observed within 158 ms (the 276 ms spectrum is shown in Figure 7I, trace B). This is explained by the fast Ni_a-SR to Ni_a-S·CO conversion according to eq 10. A small band at 1950 cm^{-1} from the Ni_a-C* state remained at about the same intensity as in the control sample. At longer times (> 20 s), this band

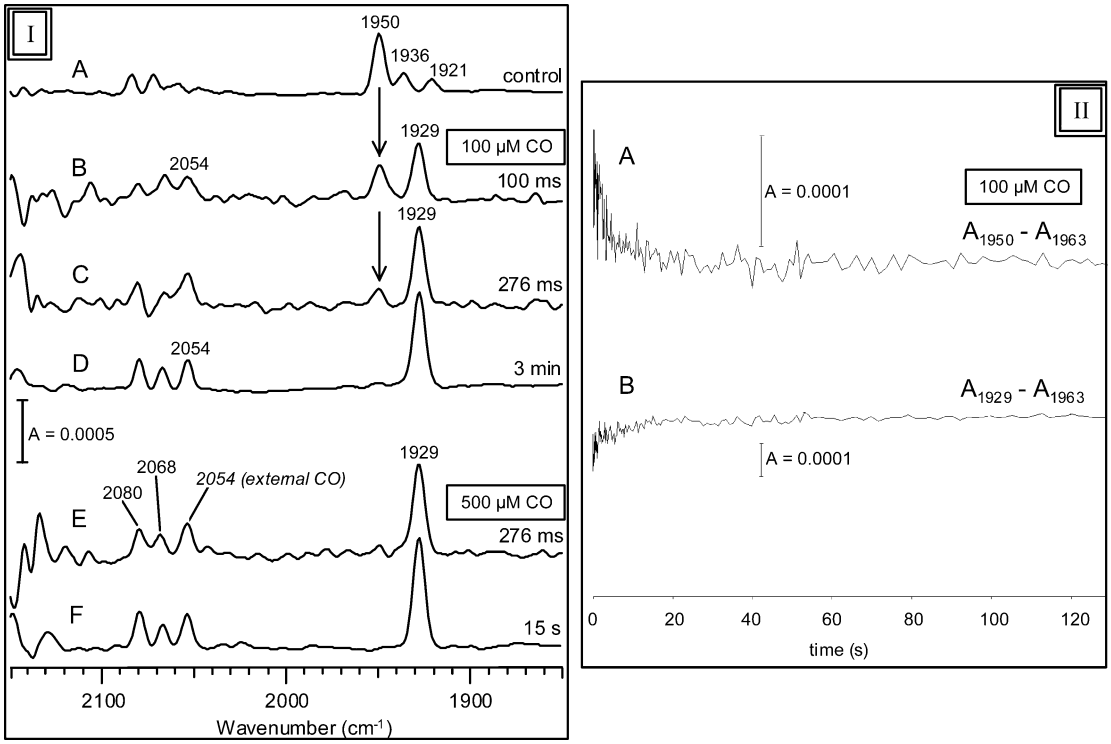

FIGURE 5: Reactions of enzyme in the Ni_a-C* state at pH 8 with two different concentrations of CO. Syringe 1 contained enzyme in the Ni_a-C* state, while syringe 2 was filled with buffer containing 200 or 1000 μM CO. Panel I: (A) Control experiment. Enzyme was mixed with anaerobic buffer, and a spectrum was recorded 3 min after mixing. (B−D) Syringe 2 contained buffer with 200 μM CO. Spectra were recorded 100 ms (B), 276 ms (C), and 3 min (D) after mixing. (E, F) Syringe 2 contained buffer with 1000 μM CO and spectra were taken after 276 ms (E) and 15 s (F). Panel II: time dependence of the amplitudes of the 1950 cm^{-1} band (A) and 1929 cm^{-1} band (B) in the experiment with 100 μM CO (absorbance at 1963 cm^{-1} used as reference).

completely disappeared. This slow decrease could be clearly seen in a 1950 minus 1963 cm^{-1} time course (not shown). The slow reaction of the 1950 cm^{-1} band (Ni_a-C*(rrr)) can be understood in terms of eq 1 with the subsequent formation of the Ni_a-S·CO(orr) state. Note that the slow reaction of the N_a-C* state is consistent with our proposal that the Ni_a-C* state is not an intermediate in the reaction of Ni_a-SR with CO (eq 10). The results are in agreement with earlier freeze-quench data (*16*), but the conclusion with respect to the reactivity of the Ni_a-SR state is not. With EPR the fast transition of Ni_a-SR to Ni_a-S·CO (eq 10) could not be followed, since both states are EPR silent. As Happe and co-workers noticed a transient increase of the Ni_a-C* signal (lost already after 40 ms), they made the assumption that the Ni_a-C* state had to be an intermediate in the conversion by CO of Ni_a-SR into Ni_a-S·CO. Hence, they came to the incorrect conclusion that the Ni_a-SR state could not react with CO.

Mixing with a 10-fold lower CO concentration (100 μM) resulted in a mixture of several states (Figure 7II). The intensity of the 1950 cm^{-1} band (Ni_a-C* state) did not change with time, not even after 30 min. The 1936/1921 cm^{-1} band from the Ni_a-SR states slightly decreased to a steady level within 276 ms and a band at 1929 cm^{-1} from the Ni_a-S·CO state appeared simultaneously. At longer times, no other changes were apparent. When the experiment was repeated with 150 μM CO in syringe 2, a higher intensity of the 1929 cm^{-1} band was observed (data not shown). Also reactions with other H_2/CO ratio's (final concentrations 720 μM H_2/75 μM CO or 670 μM H_2/165 μM CO) achieved equilibrium within 158 ms. The spectra always showed an overlap of bands as in Figure 7II, trace B, although the relative amounts were different. These data are consistent with competitive binding of H_2 and CO to Ni^{2+} in the active enzyme (eq 10). These reactions were much faster than the reaction of the Ni_a-C* state with 100 μM CO (Figure 5I, traces A and B). This is consistent with the attack of CO on the divalent nickel (Ni_a-SR state), with the concomitant release of H_2, being more facile than the attack of CO on the trivalent nickel in the Ni_a-C* state. Hydride would also be expected to bind more strongly to an Fe^{2+}-Ni^{3+} site (Ni_a-C*) than to an Fe^{2+}-Ni^{2+} site (Ni_a-SR state). Such considerations may explain the large difference in reactivity of the two states.

The fluorescent lighting in the laboratory had no effect on the reactions with CO; the IR changes and time courses of these experiments were the same in the dark.

Reactions of O_2 with the Ni_a-SR and Ni_a-C States.* Active [NiFe]-hydrogenase from *A. vinosum* is reversibly inactivated by oxygen. Addition of O_2 immediately stops hydrogen uptake by the enzyme in the presence of artificial electron acceptors in a normal activity assay, i.e., there is no noticeable Knallgas reaction. There are at least two mechanisms by which oxygen could react with reduced enzyme. First, oxygen could abstract electrons from the solvent-exposed edge of the distal [4Fe-4S] cluster. Since the reaction of H_2 with active enzyme is diffusion controlled, this would result in the reduction of O_2 with concomitant oxidation of H_2 (the Knallgas reaction). When all of the H_2 has been consumed, excess O_2 will convert the enzyme to the Ni_r*/N_u* states with the OH^-, which bridges the Ni and Fe, possibly coming from the bulk solvent. For the *A. vinosum* enzyme, this cannot be the sole mechanism of inactivation, since the enzyme does not show a Knallgas reaction. However, evidence for such a mechanism has been obtained

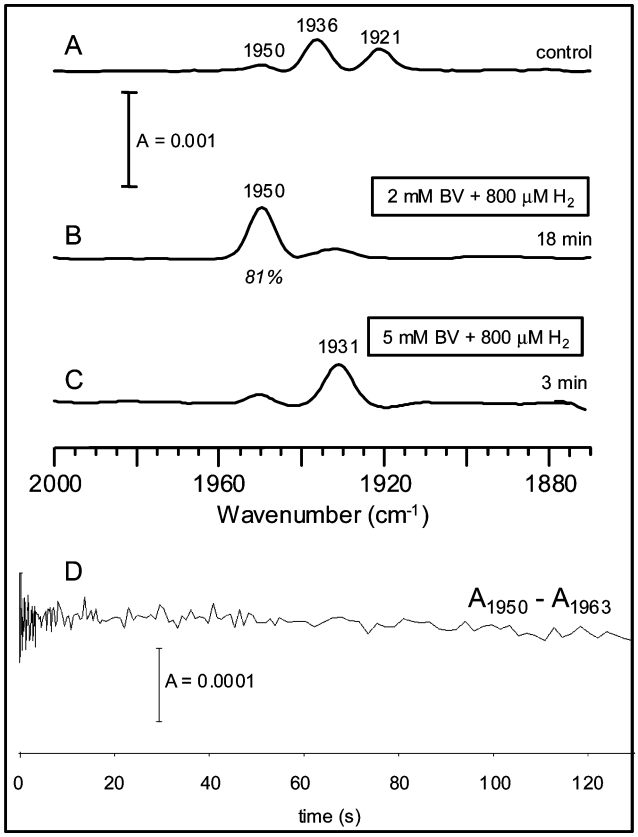

FIGURE 6: Reactions of H_2-reduced enzyme with BV in the presence of hydrogen at pH 8. Syringe 1 was filled with enzyme in buffer with 800 μM H_2. (A) Control experiment: syringe 2 contained buffer with 800 μM H_2; the spectrum was recorded 3 min after mixing. (B) Syringe 2 contained buffer with 4 mM BV and 800 μM H_2. The spectrum was taken 18 min after mixing. (C) Syringe 2 contained buffer with 10 mM BV and 800 μM H_2. The spectrum was taken after 3 min. (D) Time dependence of the amplitude of the 1950 cm^{-1} band for the experiment under B (absorbance at 1963 cm^{-1} used as a reference).

by the reoxidation of H_2-reduced *D. gigas* enzyme in $H_2{}^{17}O$ with $^{16}O_2$, where ^{17}O binding to nickel in the Ni_u* state was observed in ENDOR spectra (*30*). Such a reaction might be summarized as in eq 11.

$$Fe^{2+}(H^-)Ni^{2+}\cdot P^+M^0D^+ + 2O_2 + {}^{17}OH^- + 5H^+ \rightarrow Fe^{2+}({}^{17}OH^-)Ni^{3+}\cdot P^{2+}M^+D^{2+} + 2H_2O + H_2O_2 \quad (11)$$

A second possibility is that O_2, assuming it can enter the gas channel, reacts directly at the Ni−Fe site. When the enzyme contains two reducing equivalents or more, the likely products (peroxide or water) will be formed at the Ni−Fe site. The resulting oxidized enzyme (Ni_r* or Ni_u*) might then have an oxygen species close to nickel derived from dioxygen. Such a direct reaction would result in an immediate inactivation with respect to the reaction with H_2. As demonstrated in the accompanying paper in this issue H_2 can still react with enzyme in the Ni_r* state in the presence of oxygen. However, this reaction only results in a very slow (0.03 s^{-1}) reduction of dioxygen (*1*), which would go unnoticed in a standard activity assay.

Reoxidation of H_2-reduced *A. vinosum* hydrogenase in $H_2{}^{16}O$ by $^{17}O_2$ resulted in a ^{17}O species bound close to nickel in both the ready and unready enzyme (*14*). A reaction with enzyme containing four reducing equivalents, typically, the Ni_a-C*(orr) state, can be represented by eq 12.

$$Fe^{2+}(H^-)Ni^{3+}\cdot P^{2+}M^0D^+ + {}^{17}O_2 + 2H^+ \rightarrow Fe^{2+}({}^{17}OH^-)Ni^{3+}\cdot P^{2+}M^+D^{2+} + H_2{}^{17}O \quad (12)$$

How this would lead to either the ready or the unready state is presently unclear. In this respect, it is worthwhile to summarize the experience of the Amsterdam group in preparing the ready or unready *A. vinosum* enzyme. Quickly diluting H_2-reduced enzyme at pH 9 into O_2-saturated buffer is the best method of preparing ready enzyme in good yields (95% or more (*24*)). When performing the procedure at lower pH, or when using air-saturated buffer, more Ni_u* is always obtained. Preparation of the unready state requires quite different conditions. A good way is to take H_2-reduced enzyme at pH 6, replace the H_2 gas by CO (making predominantly the Ni_a-S·CO(oro) state), and then slowly admit O_2 (*24*). A still better method is to first add excess BV to the enzyme under CO (making the Ni_a-S·CO(oro) state in a 100% yield) and then replace the CO by O_2. Although this method also works well at pH 8, it has the disadvantage that BV is present, which is difficult to remove (Chen, M., and Albracht, S. P. J., unpublished observations; *31*).

Another way to prepare the Ni_u* state, not using CO, is to take H_2-reduced enzyme, replace the H_2 gas by Ar, add excess BV (resulting in the Ni_a-S(oro) state), and then replace the Ar by O_2 (Chen, M., and Albracht, S. P. J., unpublished; *31*). Again this procedure also works well at pH 8, but has the disadvantage of the presence of BV. It should be noted that the best methods of making the Ni_u* state utilize enzyme containing only two reducing equivalents (Ni_a-S·CO(oro) or Ni_a-S(oro) states) in the reaction with O_2. As the distal cluster is oxidized, the reaction of O_2 presumably proceeds preferentially at the Ni−Fe site with peroxide as the likely product. In this respect, it is worthwhile to mention that an irreversible loss of the enzyme activity and an associated active-site degradation occurred, when the active enzyme under CO was first treated with excess 2,6-dichlorophenol-indophenol (E'_0 = +230 mV), making a Ni_a-S(ooo) state, before CO was replaced by O_2 (van der Zwaan, J. W., Chen, M., and Albracht, S. P. J., unpublished; (*23*, *31*). As this state contains only one reducing equivalent, superoxide formation at the active site was proposed as the cause of inactivation (*23*).

(a) Reaction of the Ni_a-SR State with Oxygen. Upon mixing H_2-saturated enzyme (800 μM H_2) with oxygen-saturated buffer (1200 μM O_2) at pH 8, all of the ν(CO) bands of the reduced enzyme were replaced by one single band at 1943 cm^{-1} (Figure 7I, trace E). The reaction was complete within 160 ms (the 276 ms spectrum is shown). In the ν(CN) region two bands at 2090 and 2079 cm^{-1} were observed (data not shown). This IR spectrum is that of the Ni_r* state. This result is in agreement with earlier freeze-quench EPR experiments (*16*). Thermodynamically excess O_2 is capable of oxidizing all of the H_2 and enzyme. If both reactions would be complete within 160 ms, then the active enzyme should display a specific H_2-O_2 (Knallgas) activity (at 25 °C) of at least 127 U/mg, which is not the case. Therefore, this experiment points to involvement of a direct reaction of O_2 with the

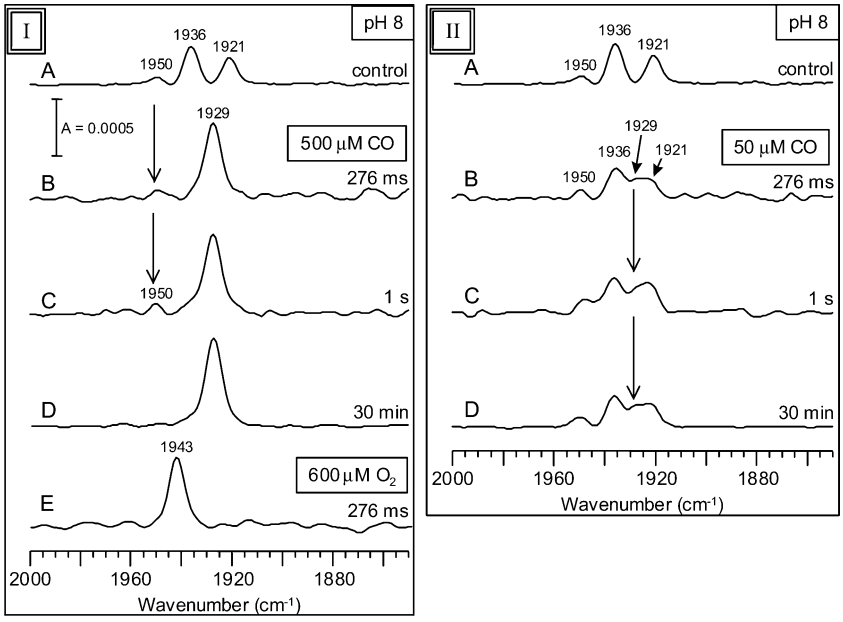

FIGURE 7: Reaction of the H_2-reduced enzyme at pH 8 with carbon monoxide or pure oxygen. Syringe 1 contained enzyme in buffer with 800 μM H_2. Syringe 2 contained buffer with 1000 μM CO (panel I, traces B−D), 1200 μM O_2 (panel I, trace E) or 100 μM CO (panel II). (A) Controls where syringe 2 contained buffer with 800 μM H_2 (spectra recorded 3 min after mixing). (B−D) Reaction with CO after 276 ms (B), 1 s (C), and 30 min (D). (E) Reaction with O_2 after 276 ms.

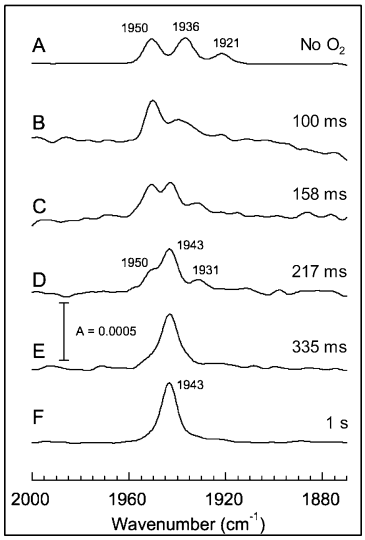

FIGURE 8: Reaction of air with enzyme in the Ni_a-SR state at pH 6. Syringe 1 contained enzyme in the Ni_a-SR state with 800 μM H_2 at pH 6. Syringe 2 was filled with air-saturated buffer (250 μM O_2). (A) Control where syringe 2 was filled with anaerobic buffer (spectrum taken after 3 min). (B−F) Spectra recorded 100 ms (B), 158 ms (C), 217 ms (D), 335 ms (E), and 1 s (F) after initiation of the reaction with oxygen.

Ni−Fe site. With excess O_2 (600 μM after mixing), the inactive Ni_r* state is formed (Figure 7I., trace E).

When using air (125 μM O_2 after mixing), however, we consistently noticed a large (2-fold or more), transient increase of the 1950 cm^{-1} band (Ni_a-C*). This was particularly obvious at pH 6. An example is given in Figure 8. The increase at 1950 cm^{-1} was complete within 100 ms; thereafter, the band collapsed within ca. 335 ms (Figure 8, traces B−E). This observation suggests that the Ni_a-C* state might be the first intermediate in the reaction of Ni_a-SR with O_2. Since the Ni_a-C* state still has bound hydride at the Ni−Fe site, we assume that this initial rapid reaction of Ni_a-SR with O_2 proceeds at the distal cluster in a two-electron reaction (eq 13).

$$Fe^{2+}(H^-)Ni^{2+}\cdot P^+M^0D^+ + O_2 + 2H^+ \rightarrow Fe^{2+}(H^-)Ni^{3+}\cdot P^{2+}M^+D^+ + H_2O_2 \quad (13)$$

As H_2 reacts extremely fast with the Ni_a-C(orr) state, the reaction with O_2 in eq 13 has to be equally fast or even slightly faster to enable an increase of steady-state concentration of Ni_a-C*. A fast H_2-oxidation (Knallgas) reaction would be expected to follow, but as already mentioned above, oxygen kills any H_2-uptake in a standard activity assay. Hence, the Ni_a-C*(orr) state, which holds four reducing equivalents, is considered to be attacked by O_2 in a subsequent slower reaction involving a direct attack at the Ni−Fe site as in eq 12. Any oxygen molecule reacting this way should inactivate one enzyme molecule. The SF-FTIR experiments indicate that the reaction in eq 12 takes between 100 and 335 ms with 125 μM O_2 and 40 μM enzyme (Figure 8). With 600 μM O_2 the reaction is faster with no observable intermediates (Figure 7I, trace E). Note that the distal Fe−S cluster has a solvent-exposed edge enabling a fast access for O_2. For reactions of H_2 and O_2 directly at the Ni−Fe site, the gases have to diffuse through the gas channel. This forms a rationale for the relative rates of the reactions. As the reaction in eq 12 becomes slower with lower oxygen concentrations, a further two-electron oxidation of the Ni_a−C*(orr) state by O_2 may occur at the distal Fe−S cluster (eq 13). It is expected that the bound hydride, the source of electrons with the lowest redox potential in this state, is then oxidized, and this would lead to the Ni_a-S(oro) state. This is how we explain the transient appearance of the 1931 cm^{-1} band in Figure 8 (traces C and D). Reaction of this state, having only two reducing equivalents, with O_2 at the Ni−Fe site is expected to produce the Ni_u* state. This may explain the asymmetry of the 1943 cm^{-1} peak in trace F of Figure 8: a contribution of the 1945 cm^{-1} band from Ni_u*.

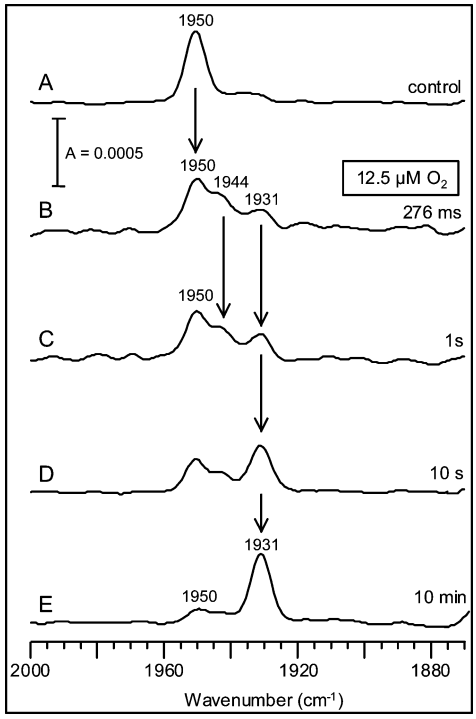

FIGURE 9: Reaction of a substoichiometric amount of oxygen with enzyme in the Ni_a-C* state at pH 6. Syringe 1 contained enzyme in the Ni_a-C* state. Syringe 2 was filled with O_2-containing buffer (25 μM O_2). (A) Control where syringe 2 was filled with anaerobic buffer (spectrum taken after 3 min). (B−E) Spectra recorded 276 ms (B), 1 s (C), 10 s (D), and 10 min (E) after mixing.

Presently, it is unclear how a peroxide close to the active site is converted to a bridging single-oxygen species as detected in the X-ray structure of the unready *D. gigas* enzyme (*32*, *33*).

(b) Reaction of the Ni_a-C State with O_2 at pH 6.* After mixing enzyme (75% in the Ni_a-C* state, 25% in the Ni_a-SR states) with air-saturated buffer (250 μM O_2), a single strong band at 1943 cm^{-1} (and ν(CN) bands at 2090 and 2079 cm^{-1}), assigned to the Ni_r* state was observed at the shortest times (100 ms; data not shown). The reaction of the Ni_a-SR is explained as in eqs 13 and 12, respectively, and the reaction of Ni_a-C as in eq 12.

When the reaction syringe contained only 25 μM O_2, then a series of slow changes were observed (Figure 9). The 1950 cm^{-1} band decreased, while two bands at 1944 and 1931 cm^{-1} appeared within 276 ms. Over the next 100 s, both the 1944 and 1950 cm^{-1} bands diminished significantly. The 1931 cm^{-1} band increased and finally became the dominant band in the spectrum.

At the start of the reaction at pH 6, the majority of the enzyme was in the Ni_a-C*(orr) state. This will react with the 12.5 μM oxygen as in eq 12. With 40 μM enzyme, this will produce a limited amount of Ni_r* with a 1943 cm^{-1} band. As the oxygen concentration is much lower than in the previous experiments, this reaction will be slower. Hence, a further oxidation via the distal cluster may proceed in two-electron steps: Ni_a-C*(orr) → Ni_a-S(oro) → Ni_u*. This will result in bands at 1931 and 1945 cm^{-1}, respectively; such bands were indeed observed within 276 ms (Figure 9, trace B). Because several bands overlap in the 1950 to 1940 cm^{-1} region, we cannot distinguish between the contributions of the Ni_r* (1943 cm^{-1}) and Ni_u* (1945 cm^{-1}) states to the 1944 cm^{-1} band.

The mixture of states (Ni_r*/Ni_u*, Ni_a-S/Ni_r-S_{1931}, and Ni_a-C*) obtained at 276 ms will subsequently come to redox equilibrium via slow intermolecular reactions. Complete reduction of 12.5 μM O_2 to water requires 50 μM reducing equivalents. With 40 μM enzyme, this means that after complete equilibration each enzyme molecule in the Ni_a-C*(orr) state should have provided one electron as shown by eq 14.

$$Fe^{2+}(H^-)Ni^{3+}\cdot P^{2+}M^0D^+ \rightarrow Fe^{2+}\text{-}Ni^{2+}\cdot P^{2+}M^0D^+ + e^- + H^+ \quad (14)$$

Formation of this Ni_a-S state is in accordance with the observed intense 1931 cm^{-1} band in the final spectrum after 10 min.

CONCLUSIONS

The first study of an [NiFe]-hydrogenase by SF-FTIR allows the following conclusions which give important new insights into the mechanisms of dihydrogen oxidation and enzyme inactivation by dioxygen (conclusions are integrated in Figure 1).

(1) The reaction of excess H_2 with enzyme in the Ni_a-S/Ni_r-S_{1931} state with both cubane clusters reduced is complete within 217 ms and directly results in the Ni_a-SR states (eq 4). If both cubane clusters are oxidized, the reaction is likewise completed within 217 ms, but now the Ni_a-SR states are formed with the Ni_a-C* state as an intermediate (eqs 7 and 8). If one cubane cluster is reduced and the other is oxidized, the reaction with H_2 results in the Ni_a-C*(rrr) state (eq 5) that cannot be rapidly converted by H_2 into the Ni_a-SR states (see point 2).

(2) Hydrogen does not react with enzyme in the Ni_a-C* state when both cubane clusters are reduced. It is concluded that an oxidized proximal cluster is essential for this reaction (eq 8). This provides a rationale for the fact that all [NiFe]-hydrogenases contain a proximal cluster in addition to the active site. Together these groups form the effective $n = 2$ redox entity that is essential for the oxidation of H_2.

(3) Enzyme in the Ni_a-S and Ni_a-SR states reacts with CO within 158 ms (eqs 9 and 10). The reaction of Ni_a-C* with CO is considerably slower (eq 1, plus the subsequent formation of Ni_a-S·CO(orr)). This is presumably because the replacement of H^- by CO on nickel is easier with Ni^{2+} (Ni_a-S and Ni_a-SR) than with Ni^{3+} (Ni_a-C*). It is concluded that the Ni_a-C* state is not an intermediate in the reaction of Ni_a-SR with CO.

(4) Oxygen can react with reduced enzyme in two ways: an extremely rapid reaction at the solvent-exposed distal [4Fe-4S] cluster and a slower reaction (100−300 ms) directly at the Ni−Fe site. The latter reaction results in the formation of the Ni_u* state (presumably with a peroxide as a product formed at the active site) or the Ni_r* state (with water formed at the active site).

(5) The data are consistent with the view that in the presence of H_2 and excess BV the Ni_a-SR → Ni_a-C* conversion is faster than the Ni_a-C* → Ni_a-S conversion. The turnover rate of the enzyme with H_2 at a pyrolytic graphite electrode is diffusion controlled and much higher

than any routine H_2-A activity assay (A = artificial electron acceptor) (*19*, *20*). This indicates that during the H_2−BV reaction the enzyme presumably cycles between the Ni_a-C*-(orr) and Ni_a-SR(rrr) states (eq 8). If the H_2 concentration becomes very low, as often found in natural habitats of H_2-metabolizing bacteria, then the Ni_a-S to Ni_a-C* transition (eq 5) may be the main redox shuttle.

REFERENCES

1. Kurkin, S., George, S. J., Thorneley, R. N. F., and Albracht, S. P. J. (2004) Hydrogen-induced activation of the [NiFe]-hydrogenase from *Allochromatium vinosum* as studied by stopped-flow infrared spectroscopy, *Biochemistry 43*, 6820−6831.
2. George, S. J., Ashby, G. A., Wharton, C. W., and Thorneley, R. N. F. (1997) Time-resolved binding of carbon monoxide to nitrogenase monitored by stopped-flow infrared spectroscopy, *J. Am. Chem. Soc. 119*, 6450−6451.
3. Thorneley, R. N. F., and George, S. J. (2000) in *Prokaryotic Nitrogen Fixation: A Model System for Analysis of a Biological Process* (Triplett, E. W., Ed.) pp 81−100, Horizon Scientific Press, Wymondham, U.K.
4. Muthusamy, M., Ambundo, E. A., George, S. J., Lippard, S. J., and Thorneley, R. N. F. (2003) Stopped-flow Fourier transform infrared spectroscopy of nitromethane oxidation by the diiron-(IV) intermediate of methane monooxygenase, *J. Am. Chem. Soc. 125*, 11150−11151.
5. Cammack, R., Patil, D. S., Hatchikian, E. C., and Fernández, V. M. (1987) Nickel and iron-sulphur centres in *Desulfovibrio gigas* hydrogenase: ESR spectra, redox properties and interactions, *Biochim. Biophys. Acta 912*, 98−109.
6. Van der Zwaan, J. W., Albracht, S. P. J., Fontijn, R. D., and Slater, E. C. (1985) Monovalent nickel in hydrogenase from *Chromatium vinosum*. Light sensitivity and evidence for direct interaction with hydrogen, *FEBS Lett. 179*, 271−277.
7. Coremans, J. M. C. C., van Garderen, C. J., and Albracht, S. P. J. (1992) On the redox equilibrium between H_2 and hydrogenase, *Biochim. Biophys. Acta 1119*, 148−156.
8. Barondeau, D. P., Roberts, L. M., and Lindahl, P. A. (1994) Stability of the Ni−C state and oxidative titrations of *Desulfovibrio-gigas* hydrogenase monitored by EPR and electronic absorption spectroscopies, *J. Am. Chem. Soc. 116*, 3442−3448.
9. Pierik, A. J., Schmelz, M., Lenz, O., Friedrich, B., and Albracht, S. P. J. (1998) Characterization of the active site of a hydrogen sensor from *Alcaligenes eutrophus*, *FEBS Lett. 438*, 231−235.
10. Bernhard, M., Buhrke, T., Bleijlevens, B., De Lacey, A. L., Fernandez, V. M., Albracht, S. P. J., and Friedrich, B. (2001) The H_2 sensor of *Ralstonia eutropha*. Biochemical characteristics, spectroscopic properties, and its interaction with a histidine protein kinase, *J. Biol. Chem. 276*, 15592−15597.
11. Cammack, R., Frey, M., and Robson, R. (2001) *Hydrogen as a Fuel. Learning from Nature*, Taylor & Francis Inc., New York.
12. Foerster, S., Stein, M., Brecht, M., Ogata, H., Higuchi, Y., and Lubitz, W. (2003) Single-crystal EPR studies of the reduced active site of [NiFe] hydrogenase from *Desulfovibrio vulgaris* Miyazaki F, *J. Am. Chem. Soc. 125*, 83−93.
13. Van der Zwaan, J. W., Albracht, S. P. J., Fontijn, R. D., and Roelofs, Y. B. M. (1986) EPR evidence for direct interaction of carbon monoxide with nickel in hydrogenase from *Chromatium vinosum*, *Biochim. Biophys. Acta 872*, 208−215.
14. Van der Zwaan, J. W., Coremans, J. M. C. C., Bouwens, E. C., and Albracht, S. P. J. (1990) Effect of $^{17}O_2$ and ^{13}CO on EPR spectra of nickel in hydrogenase from *Chromatium vinosum*, *Biochim. Biophys. Acta 1041*, 101−110.
15. Sorgenfrei, O., Duin, E. C., Klein, A., and Albracht, S. P. J. (1996) Interactions of ^{77}Se and ^{13}CO with nickel in the active site of active F_{420}-nonreducing hydrogenase from *Methanococcus voltae*, *J. Biol. Chem. 271*, 23799−23806.
16. Happe, R. P., Roseboom, W., and Albracht, S. P. J. (1999) Pre-steady-state kinetics of the reactions of [NiFe]-hydrogenase from *Chromatium vinosum* with H_2 and CO, *Eur. J. Biochem. 259*, 602−608.
17. Bagley, K. A., Van Garderen, C. J., Chen, M., Duin, E. C., Albracht, S. P. J., and Woodruff, W. H. (1994) Infrared studies on the interaction of carbon monoxide with divalent nickel in hydrogenase from *Chromatium vinosum*, *Biochemistry 33*, 9229−9236.
18. Ogata, H., Mizoguchi, Y., Mizuno, N., Miki, K., Adachi, S., Yasuoka, N., Yagi, T., Yamauchi, O., Hirota, S., and Higuchi, Y. (2002) Structural studies of the carbon monoxide complex of [NiFe]hydrogenase from *Desulfovibrio vulgaris* Miyazaki F: suggestion for the initial activation site for dihydrogen, *J. Am. Chem. Soc. 124*, 11628−11635.
19. Pershad, H. R., Duff, J. L. C., Heering, H. A., Duin, E. C., Albracht, S. P. J., and Armstrong, F. A. (1999) Catalytic electron transport in *Chromatium vinosum* [NiFe]-hydrogenase: Application of voltammetry in detecting redox-active centers and establishing that hydrogen oxidation is very fast even at potentials close to the reversible H^+/H_2 value, *Biochemistry 38*, 8992−8999.
20. Jones, A. K., Sillery, E., Albracht, S. P. J., and Armstrong, F. A. (2002) Direct comparison of the electrocatalytic oxidation of hydrogen by an enzyme and a platinum catalyst, *Chem. Commun.* 866−867.
21. Coremans, J. M. C. C., van der Zwaan, J. W., and Albracht, S. P. J. (1992) Distinct redox behaviour of prosthetic groups in ready and unready hydrogenase from *Chromatium vinosum*, *Biochim. Biophys. Acta 1119*, 157−168.
22. George, S. J., Armstrong, F. A., Hatchikian, E. C., and Thomson, A. J. (1989) Electrochemical and spectroscopic characterization of the conversion of the 7Fe into the 8Fe form of ferredoxin III from *Desulfovibrio africanus*. Identification of a [4Fe-4S] cluster with one noncysteine ligand, *Biochem. J. 264*, 275−284.
23. Albracht, S. P. J. (1994) Nickel hydrogenases: in search of the active site, *Biochim. Biophys. Acta 1188*, 167−204.
24. Bleijlevens, B. (2001) The hydrogen-consumption activity of the [NiFe] hydrogenase of *Allochromatium vinosum* in different redox states, in *Hydrogen as a Fuel. Learning from Nature* (Cammack, R., Frey, M., and Robson, R., Eds.) pp 82−84, Taylor & Francis, London.
25. Surerus, K. K., Chen, M., van der Zwaan, J. W., Rusnak, F. M., Kolk, M., Duin, E. C., Albracht, S. P. J., and Münck, E. (1994) Further characterization of the spin coupling observed in oxidized hydrogenase from *Chromatium vinosum*. A Mössbauer and multifrequency EPR study, *Biochemistry 33*, 4980−4993.
26. Duin, E. C. (1996) Exploring the active site of nickel−hydrogenases, Ph.D. Thesis, University of Amsterdam.
27. Van der Zwaan, J. W., Albracht, S. P. J., Fontijn, R. D., and Mul, P. (1987) On the anomalous temperature behaviour of the EPR signal of monovalent nickel in hydrogenase, *Eur. J. Biochem. 169*, 377−384.
28. Albracht, S. P. J. (2001) Spectroscopy − the functional puzzle, in *Hydrogen as a Fuel. Learning from Nature* (Cammack, R., Frey, M., Robson, R., Eds.) pp 110−158, Taylor & Francis, London.
29. De Lacey, A. L., Hatchikian, E. C., Volbeda, A., Frey, M., Fontecilla-Camps, J. C., and Fernandez, V. M. (1997) Infrared spectroelectrochemical characterization of the [NiFe] hydrogenase of *Desulfovibrio gigas*, *J. Am. Chem. Soc. 119*, 7181−7189.
30. Carepo, M., Tierney, D. L., Brondino, C. D., Yang, T. C., Pamplona, A., Telser, J., Moura, I., Moura, J. J. G., and Hoffman, B. M. (2002) ^{17}O ENDOR detection of a solvent-derived Ni-(OH_x)-Fe bridge that is lost upon activation of the hydrogenase from *Desulfovibrio gigas*, *J. Am. Chem. Soc. 124*, 281−286.
31. Chen, M. (1992) Hydrogenase from *Chromatium vinosum*. Function and reactivity of metal centres, Ph.D. Thesis, University of Amsterdam, Amsterdam, The Netherlands.
32. Volbeda, A., Charon, M. H., Piras, C., Hatchikian, E. C., Frey, M., and Fontecilla-Camps, J. C. (1995) Crystal structure of the nickel−iron hydrogenase from *Desulfovibrio gigas*, *Nature 373*, 580−587.
33. Volbeda, A., Garcia, E., Piras, C., deLacey, A. L., Fernandez, V. M., Hatchikian, E. C., Frey, M., and Fontecilla-Camps, J. C. (1996) Structure of the [NiFe] hydrogenase active site: Evidence for biologically uncommon Fe ligands, *J. Am. Chem. Soc. 118*, 12989−12996.
34. Bleijlevens, B. (2002) Activation and sensing of hydrogen in nature, Ph.D. Thesis, University of Amsterdam, Amsterdam (ISBN: 90−9016166-x).

BI049853K